BEHAVIOUR OF GROUND ANCHORS IN STIFF CLAYS

Comportement de tirants d'ancrage en argiles raides

by

Aldo EVANGELISTA
and
Giovanni SAPIO

Resp. Assistant Professor and Professor of Geotechnics, University of Naples, Italy

SOMMAIRE

La communication présente les résultats in situ sur des ancrages dans une argile pliocène à Taranto (Italie). Les résultats ont été analysés théoriquement par un calcul numérique basé sur un demi-espace élastique isotrope en tenant compte du déplacement relatif à la surface de contact structure-sol.

Traditionnellement, la fissuration du mortier d'injection est prise en considération. En se basant sur cette analyse, on obtient des valeurs caractéristiques du sol et de l'ancrage qui s'accordent le mieux avec le résultat expérimental. Elles sont comparées avec des valeurs, parfois différentes, obtenues par les essais normaux en laboratoire.

Finalement, l'importance de la fissuration du mortier d'injection est soulignée.

SUMMARY

The results of a full scale investigation on instrumented anchors, bored through a typical pliocenic stiff clay formation, are reported and analyzed. The variation with depth of the normal stress in the reinforcement bars, found to be non-linear up to failure load, is predicted by a non-linear numerical analysis of the interaction among the reinforcement, the grout mortar and the surrounding soil taking into account the cracking of the mortar. The best correlation with experimental results, however, is obtained with values of soil and mortar properties somewhat different from laboratory values.

A similar correlation of load-upheaval curves has been obtained, by the same analysis and with the same values of parameters, only for the first stage of the curves and not for the final stage, near to failure load.

This inconsistency is discussed, pointing out the need for further theoretical and experimental investigations.

1. INTRODUCTION

In a recent paper (Sapio, 1975) the results of a full scale investigation on 3 test anchors bored through a typical pliocenic clay formation of Southern Italy were reported.

Calling τ_{av} the average adhesion at failure between the grouted length of the anchor and the soil, and c_u the undrained cohesion of the soil as measured in laboratory tests on undisturbed samples, values of the ratio $\alpha = \tau_{av}/c_u$ ranging between 0.28 and 0.36 were measured (see table I).

In the mean time, the values of normal stress in the reinforcement bars were measured by means of strain gauges, glued to the bars at different depths.

The stress variation with depth was far from linear not only at low stress level, as found for instance by Berardi (1967) and Adams and Klym (1972), but also at failure.

Such a finding is in contrast with the usual hypothesis of uniform shear stress distribution on the lateral surface of the anchor at failure. Accordingly,

TABLE I

Anchor	Nominal diameter ∅ mm	Grouted length L m	Depth below ground level m	Ultimate uplift load Q_f tons	Adhesion coefficient α
A	220	3.80	7.20 ÷ 11.00	20	0.28
B	220	7.20	7.80 ÷ 15.00	50	0.36
C	220	12.80	6.20 ÷ 19.00	80	0.33

the need for a further analysis of the behaviour of the anchors was underlined, considering the mutual interaction of the steel bars, the grout and the surrounding soil.

A step towards this goal is attempted in this paper; only two of the three anchors are considered, since in the third one the strain gauges failed at the beginning of the uplift test.

2. FIELD INVESTIGATION

2.1. Subsoil properties

Field experiences were carried out at Taranto (Italy) in a formation of overconsolidated stiff clays of pliocenic age, typical of the region (Apulia), where it is found in wide areas with rather uniform characteristics.

At the test site the formation is overlain by overburden soils, for a thickness of 3.5 m, and by a layer of partially cemented sand 2 m thick.

The clay is of medium to high plasticity; its grain size distribution is reported in fig. 1.

Physical properties, as determined on undisturbed samples, are listed in table II. Typical oedometer curves are reported in fig. 2; as it may be seen, the clay appears to be heavily overconsolidated.

Undrained stress-strain and strength properties were obtained by means of unconsolidated undrained triaxial compression test; relevant results are listed in table III.

TABLE II

Physical properties of clays from lab. tests

Sample	Depth (m)	Porosity n %	Water content w %	Unit weigth γ t/m³
1	7.50 ÷ 7.90	45.7	30.8	1.94
2	9.80 ÷ 10.20	38.5	22.9	2.06
3	12.00 ÷ 12.40	36.5	21.0	2.10
A	13.45 ÷ 13.75	37.5	22.0	2.08
4	14.20 ÷ 14.60	40.6	24.1	2.01
B	14.70 ÷ 15.10	39.9	24.3	2.04
6	20.60 ÷ 21.00	37.1	20.6	2.07
7	25.00 ÷ 25.40	38.6	22.9	2.06
averages		39.3	23.6	2.05

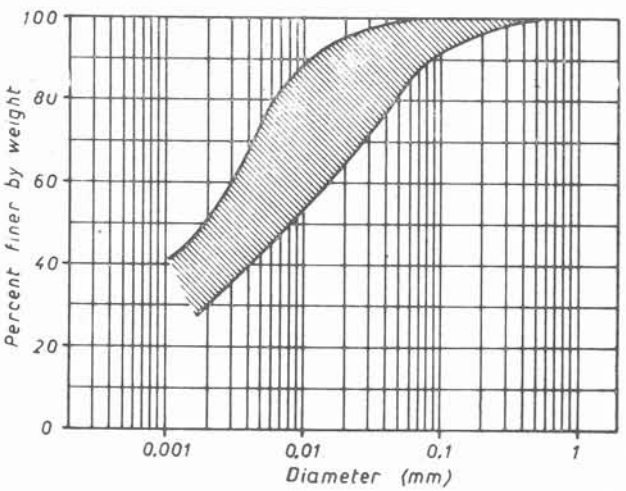

Fig. 1. — **Grain size distribution of clay.**

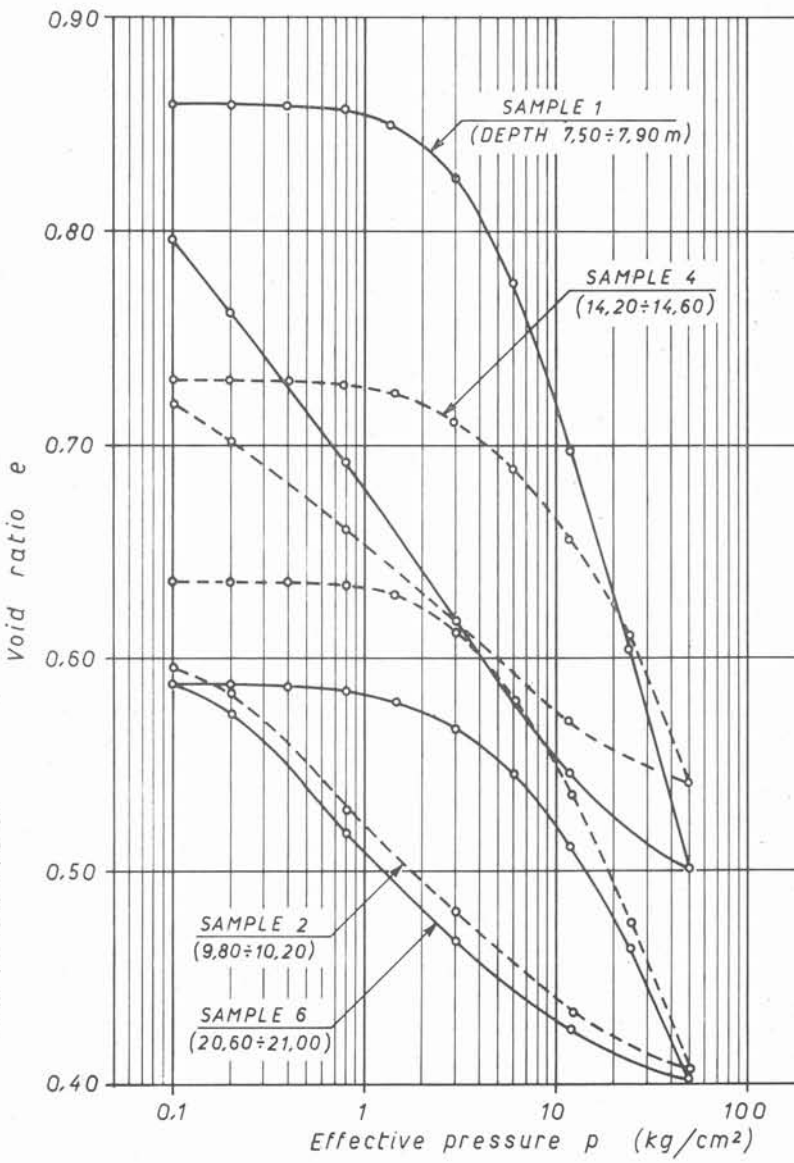

Fig. 2. — **Œdometer curves of clay.**

Stress-strain curves were fitted by a hyperbola (Kondner and Zelasko, 1963), fig. 3 a, whose parameters $a = 1/E_i$ and $b = 1/(\sigma_1 - \sigma_3)_u$ were obtained by the linear plot of $\varepsilon/(\sigma_1 - \sigma_3)$ versus ε (fig. 3 b). Initial undrained tangent modulus E_i ranges between 166 and 500 kg/cm²; the ultimate deviator stress $(\sigma_1 - \sigma_3)_u$ derived by the hyperbolic interpolation is, on the average, 14% higher than the deviator stress at failure $(\sigma_1 - \sigma_3)_f$. The fitting obtained with the hyperbola is rather good, as it may be seen in fig. 3 b.

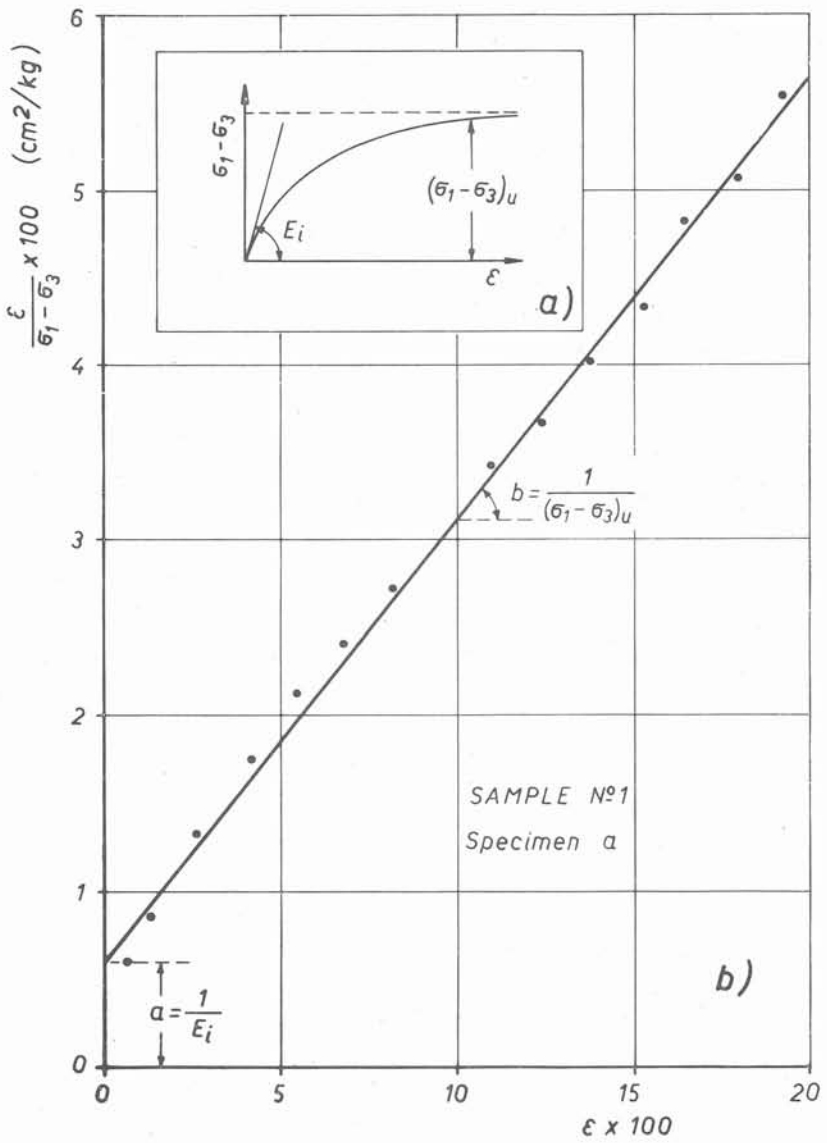

Fig. 3. — **Triaxal compression tests. Stress-strain curves fitting by a hyperbola.**

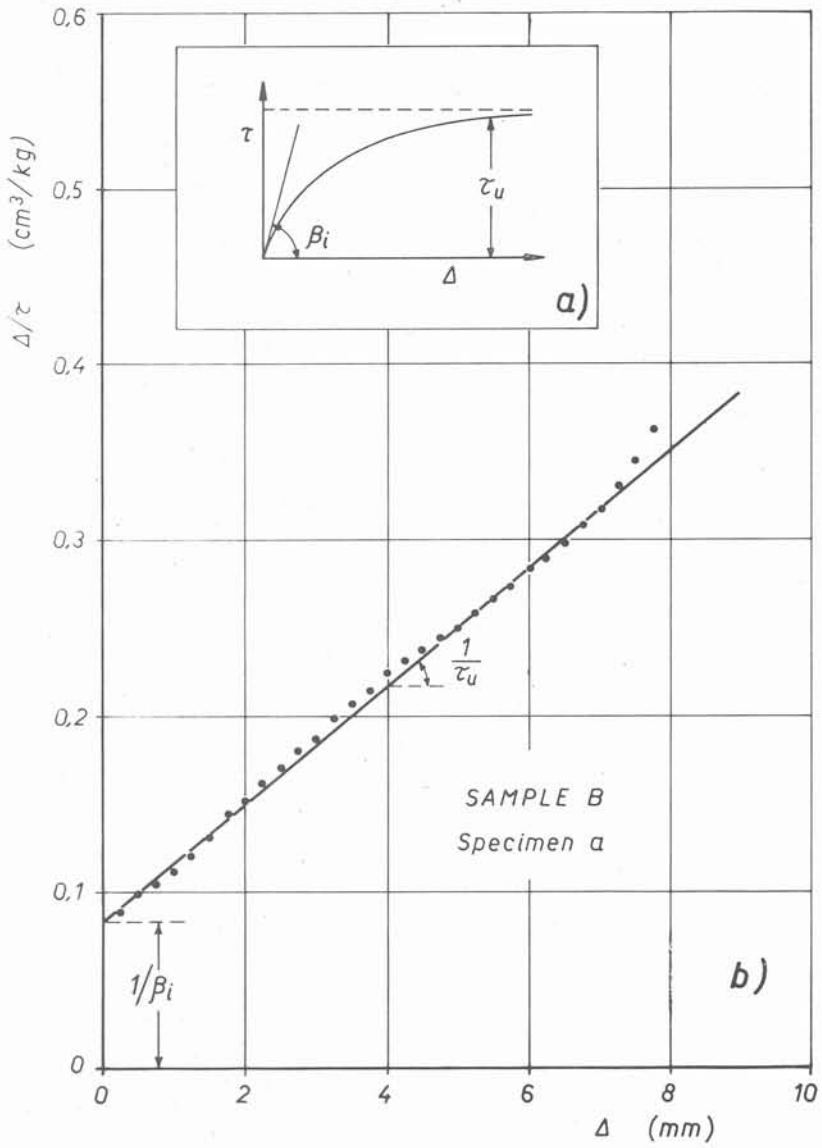

Fig. 4. — **Shear box tests. Stress-strain curves fitting by a hyperbola.**

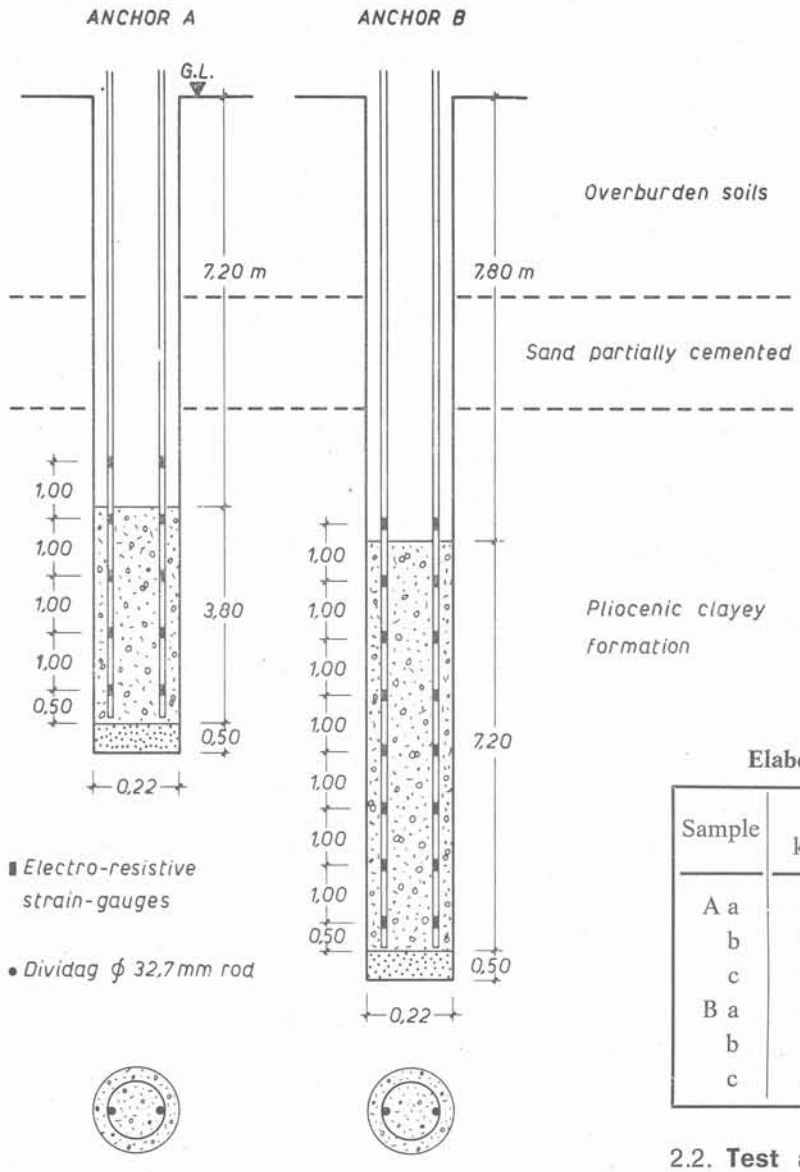

Fig. 5 — **Test anchors.**

Note: widths not in scale

Some unconsolidated undrained shear box tests were also performed; typical results are listed in table IV. A hyperbolic interpolation was attempted for these tests (fig. 4); the values of initial tangent modulus β_i and ultimate strength τ_u thus obtained are also reported in table IV.

A comparison between tables III and IV shows that the hyperbolic interpolation is more suited for triaxial than for direct shear test results.

TABLE III

Elaboration of the triaxial compression test results

Sample	E_i kg/cm²	$(\sigma_1 - \sigma_3)_u$ kg/cm²	$(\sigma_1 - \sigma_3)_f$ kg/cm²	$\frac{(\sigma_1 - \sigma_3)_u}{(\sigma_1 - \sigma_3)_f}$
1 a	166	4.00	3.55	1.13
b	200	3.13	2.88	1.09
c	227	3.45	3.06	1.13
3 a	208	7.14	5.98	1.19
b	263	7.69	6.65	1.16
6 a	500	7.14	6.35	1.12
b	500	7.14	6.30	1.13
c	385	7.14	6.03	1.18

TABLE IV

Elaboration of the shear box test results

Sample	β_i kg/cm³	τ_u kg/cm²	τ_f kg/cm²	τ_u/τ_f
A a	10.17	2.88	2.34	1.23
b	10.75	3.52	2.37	1.48
c	11.49	3.97	2.44	1.63
B a	11.90	2.99	2.23	1.34
b	12.50	4.67	2.98	1.57
c	13.51	3.79	2.64	1.44

2.2. Test anchors

The two anchors considered in this paper are represented in fig. 5. The first one (anchor A) has a grouted length of 3.8 m and a total length of 11 m; the second one (anchor B), respectively of 7.2 m and 15 m.

Both anchors were drilled with rotary bit and a provisional steel casing 220 mm in diameter. At the bottom of the hole, a layer of fine sand, 50 cm thick, was poured before introducing the reinforcement, that consists of two Dividag rods 32.7 mm in diameter fastened to spacing rings.

The bars are instrumented with strain gauges as shown in fig. 5.

The grout mortar was obtained by mixing 1 m³ of fine sand, 1 200 kg of R. 325 cement and 800 l of water; it was poured through a tremie pipe lowered to the hole bottom.

During the mortar casting, the steel casing was progressively raised and finally left in place above the grouted length of the anchor.

Some specimens, prepared in laboratory with the same mix used in the field, gave the following average 28 days strength:

compression strength : 310 kg/cm²
bending strength : 36 kg/cm²

The reinforcement steel has the following characteristics:

yield-stress : 86×10^2 kg/cm²

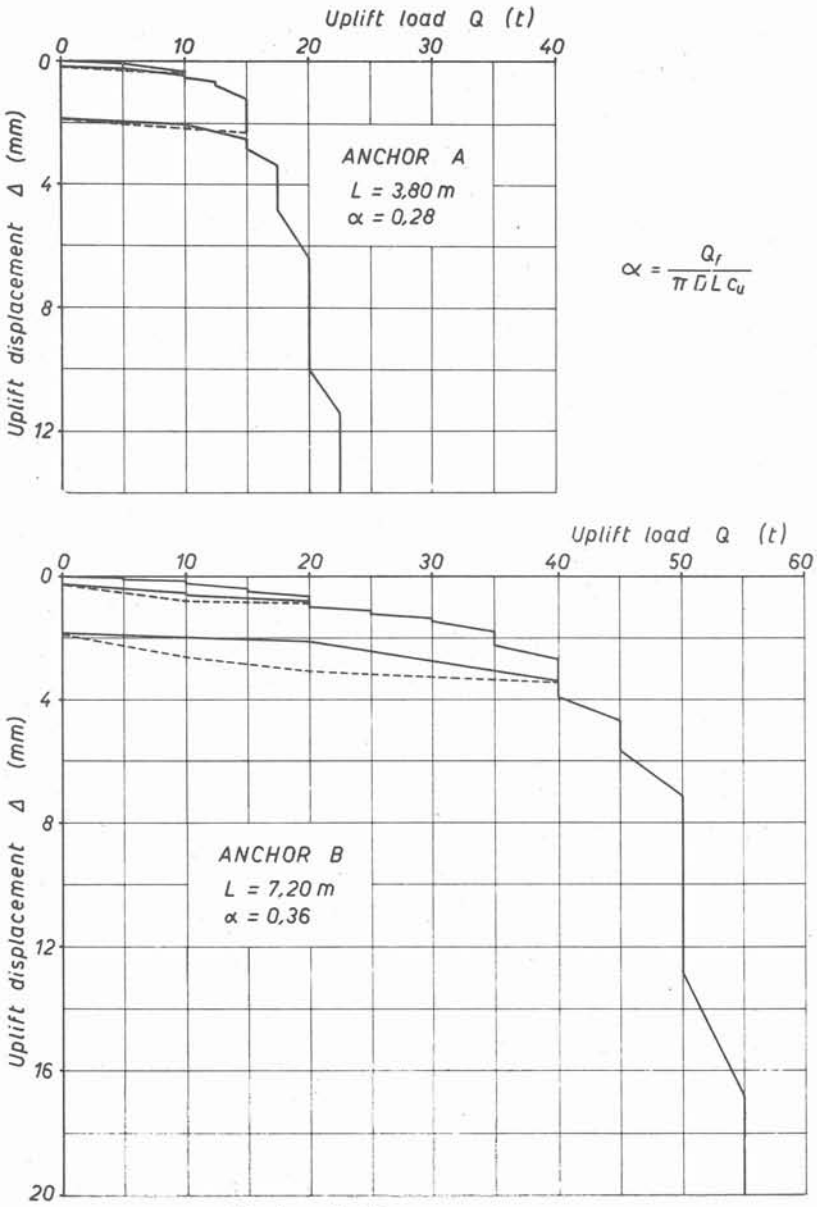

Fig. 6. — **Uplift test results.**

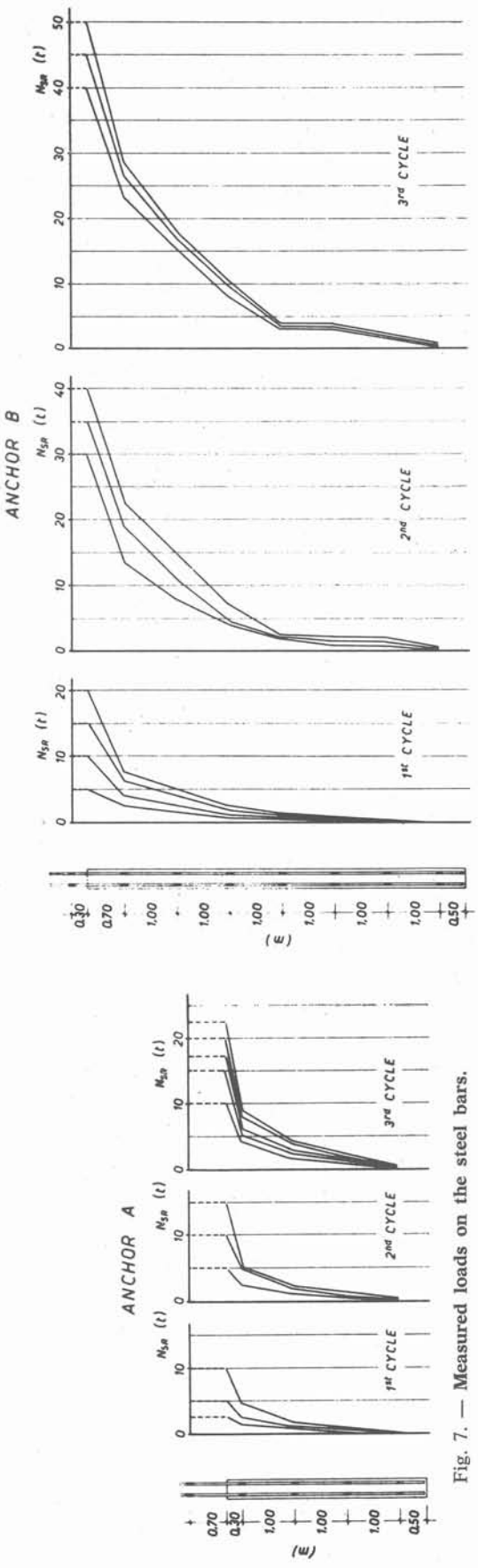

Fig. 7. — **Measured loads on the steel bars.**

tensile strength : 105×10^2 kg/cm²
Young's modulus : 2.2×10^6 kg/cm²

The anchors were constructed by Fondedile S.p.A., Naples.

2.3. Uplift tests

Uplift tests were carried out nearly two months after the construction of the anchors. The load was applied by means of a couple of hydraulic jacks, via a test frame with a 100 ton capacity. The displacements were measured by means of 4 dial gauges, and independently by optical levelling.

Three loading and unloading cycles were performed for each test, the last one kept to failure load.

The results obtained are shown in fig. 6 as curves of the vertical displacement Δ versus applied uplift load Q. The load distribution on the stell bars, derived from the strain gauges readings, is reported in fig. 7. As already said, such a distribution is non-linear up to the ultimate uplift load.

3. THEORETICAL INTERPRETATION

3.1. Hypothesis

To interpret the observed behaviour of the test anchors, the subsoil was treated as a homogeneous, isotropic, elastic half space, except for a thin layer surrounding the anchor where yield may eventually occur.

Yield occurrence, in terms of total stress, has been postulated when the shear stress at the interface between the anchor and the soil reaches a limit value; this yield stress has been assumed to be constant over the anchor length and function of the undrained cohesion of the soil.

In the calculation the above mentioned thin layer was assumed to coincide with the interface between the grout and the soil; shear displacement at this interface was related to corresponding shear stress by a hyperbolic law.

The overall conditions being undrained, a Poisson's ratio equal to 0.5 was assumed for the soil.

The anchor body was treated as a homogeneous body whose deformability equals that of the grout-reinforcement system. Moreover, the occurrence of tension cracks in the upper part of the anchor was considered by assuming that, if the tensile stress in the grout exceeds the tensile strength, the normal load is resisted only by the steel reinforcement while the surrounding grout keeps the only function of transmitting the shear stress from the soil to the reinforcement.

3.2. Calculation procedures

The calculation procedure adopted is based on the discretization procedure developed for the study of pile foundations (Poulos and Davis, 1968; Mattes and Poulos, 1969; Evangelista, 1976); the anchor, actually, may be treated as a pile with a non-reacting base.

According to such procedures, the anchor was subdivided into K elements; for the i-th element an equation containing the unknown shear stresses on all the K elements and the displacement of the i-th element may be written. A further equation is obtained by the condition of overall vertical equilibrium. In matrix form, the displacement Δ_s of the soil corresponding to the K elements are connected to the interface shear stresses τ by the equation:

$$\{\Delta_s\} = [S]\,\{\tau\}$$

where [S] represents the matrix of the influence coefficients of the soil, obtained by numerical integration of Mindlin's formula. Calling Δ_o the displacement of the soil at the anchor base, and putting

$$\{\Delta'_s\} = \{\Delta_s\} - \Delta_o$$

this can be expressed:

$$\{\Delta'_s\} = [S']\,\{\tau\}$$

The displacements Δ_a of the elements of the anchor, under the action of the axial load Q and of the tangential stress $-\tau$ may be written:

$$\{\Delta_a\} = \Delta_o + \Delta_b - [A]\,\{\tau\} + \{\Delta^Q\}$$

where Δ_b is the unknown mutual displacement between the grout and the soil at the anchor base (fig. 8); the term $-[A]\,\{\tau\}$ represents the deformation of the anchor due to the stress $-\tau$; $\{\Delta^Q\}$ represents the deformation due to the load Q.

To construct matrix [A] and to calculate deformations $\{\Delta^Q\}$, the anchor was considered as a homogeneous cylinder. If tension cracks occur, the anchor has an equivalent modulus E_1 in the fissured zone, and a different modulus E_2 in the unfissured one. They are expressed respectively:

$$E_1 = \frac{4\,E_{SR}\,\Omega_{SR}}{\pi\,D^2}\;;\; E_2 = \frac{4\,(E_{SR}\,\Omega_{SR} + E_M\,\Omega_M)}{\pi\,D^2}$$

where:

E_{SR}, Ω_{SR}, the Young's modulus and the total area of reinforcement bars;

E_M, Ω_M, the Young's modulus and the area of the mortar;

D, the nominal diameter of the anchor.

Of course, the length of the cracked zone is unknown, and must be determined.

The compatibility equations are expressed:

$$\{\Delta_a\} = \{\Delta_s\} + \{\delta\} \qquad (1)$$

where $\{\delta\}$ represents the shear displacement between the mortar and the soil. By substituting:

$$([S'] + [A])\,\{\tau\} = \Delta_b + \{\Delta^Q\} - \{\delta\} \qquad (2)$$

The displacement δ was related to the shear stress at the interface by a hyperbolic equation of the type:

$$\delta_i = \frac{1}{\beta}\,\frac{\tau_i}{1 - \tau_i/\tau_a} \qquad (3)$$

where β is the initial gradient of the τ, δ curve, and τ_a is the asymptotic limit value of τ_i. A similar interface behaviour has been used by Clough and Duncan (1971) and by Desai (1974).

The équilibrium equation is expressed:

$$Q = [B]\,\{\tau\}$$

that is

$$\frac{\pi\,DL}{K}\sum_{i=1}^{K}\tau_i = Q \qquad (4)$$

Eqs. (2) and (4) offer the solution to the problem.

Eq. (3) being non linear, the whole system is non linear; it has been solved in increments, by considering loading steps ΔQ and writing eq. (3) in incremental form:

$$\Delta\,\delta_i = \frac{1}{\beta}\,\frac{\Delta\,\tau_i}{(1 - \tau_i/\tau_a)^2}$$

τ_i being the value of the interface shear stress just before the load increment ΔQ. Since matrix [A] and vector $\{\Delta^Q\}$ vary with the length of cracked zone, after each loading step the occurrence and the extent of this zone is checked, and [A] and $\{\Delta^Q\}$ are eventually recalculated.

The solution of the system (2) and (4) gives the K values of τ_i; simple equilibrium considerations allow then the determination of the axial load N in any section of the anchor.

The fraction N_{SR} of N taken up by the steel bars in the uneracked length is:

$$N_{SR} = N\,\frac{E_{SR}\,\Omega_{SR}}{E_{SR}\,\Omega_{SR} + E_M\,\Omega_M}$$

On the contrary, in the cracked length the value of N_{SR} is unknown, the location of the cracks being unknown. Nevertheless, the range of possible values of N_{SR} may be defined; they vary between a minimum $N_{SR\,min}$ (fig. 9) occurring if the mortar fully develops its tensile strength, and a maximum $N_{SR\,max}$ corresponding to a fully cracked mortar. Of course, one may write:

$$N_{SR\,min} = N - \sigma_{FM}\,\Omega_M;\; N_{SR\,max} = N$$

where σ_{FM} is the tensile strength of the mortar.

Fig. 8. — **Displacement symbolism.**

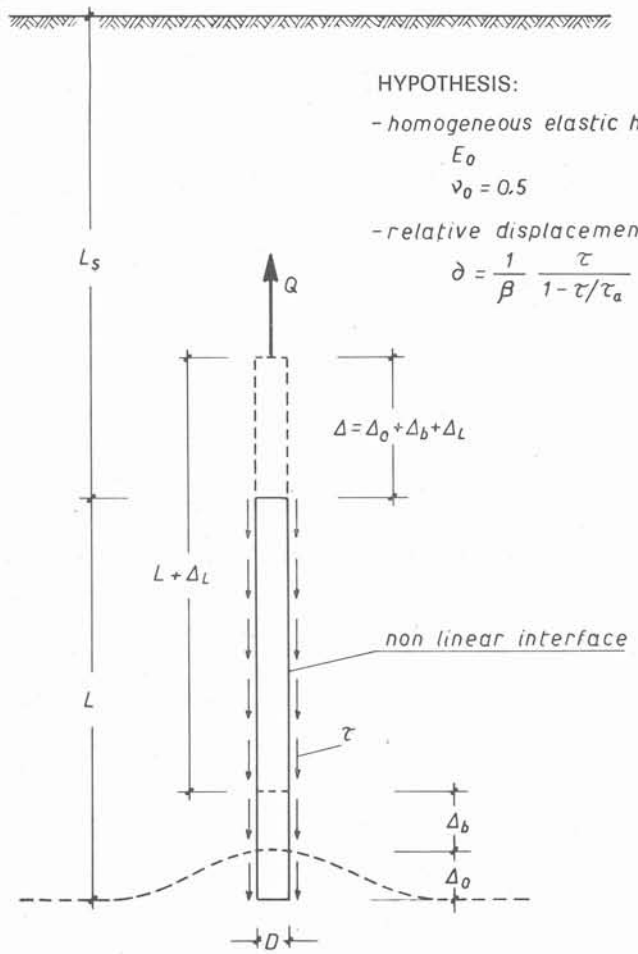

Finally, the displacement Δ of the anchor's head was obtained (fig. 8) as the sum of: the upheaval Δ_o of the soil below the anchor; the displacement Δ_b between the soil and the base of the anchor; the increase Δ_L of the anchor's length.

Δ_o has been calculated by integration of Mindlin expressions, once the tangential stresses $\{\tau\}$ known.

3.3. Results and discussion

In order to compare the experimental results with those obtained in the calculations, the following physical parameters must be known;

- Length L, diameter D and depth L_s of the anchor;
- Percentage of reinforcement, expressed by the ratio Ω_{SR}/Ω_M;
- Undrained modulus of the soil E_o;
- Young's modulus of the steel. E_{SR}, and of the mortar, E_M, in tension;
- σ_{FM} = tensile strength of the mortar;
- β = initial tangent to the curve connecting shear stress τ and displacement δ at the interface between mortar and soil;
- τ_a = limit value of τ, corresponding to the asymptote of the $\tau - \delta$ curve.

Besides geometrical parameters, the only defined property is the Young's modulus of the steel bars, that was determined in the usual way and equals 2.2×10^6 kg/cm^2.

Laboratory values of E_M and σ_{FM} are respectively of the order of 2×10^5 kg/cm^2 and 30 kg/cm^2; they have been assumed as valid in the calculations, notwithstanding the obvious differences in curing conditions between the laboratory and the site.

E_o, β and τ_a have been determined, by trial and error, on the basis of best correlation to experimental results.

As a first trial, E_o was assumed equal to the mean value of E_i (table III) and β to the mean value of β_i (table IV).

τ_a was assumed: $\tau_a = \alpha\, c_u$, with c_u taken from laboratory measurements (table III and IV) and α (adhesion coefficient) from table I ($\alpha = 0.28$ for anchor A; 0.36 for anchor B).

The results thus obtained being unsatisfactory, successive trials have shown that a reasonably good correlation is obtained by assuming:

$E_o = 700$ kg/cm^2; $\beta = 50$ kg/cm^3;
$\tau_a = 2.75$ kg/cm^2.

Fig. 9. — **Possible load distribution on the steel bars.**

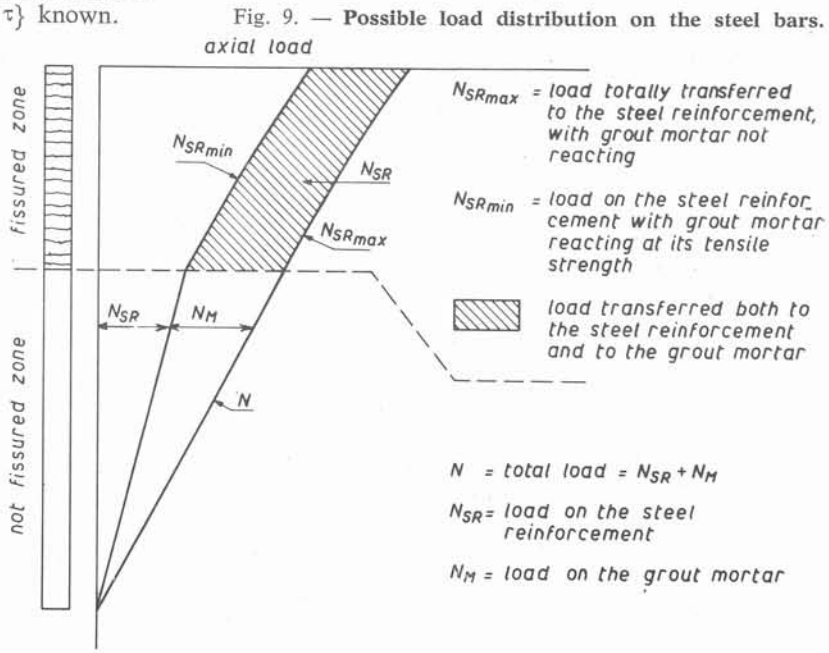

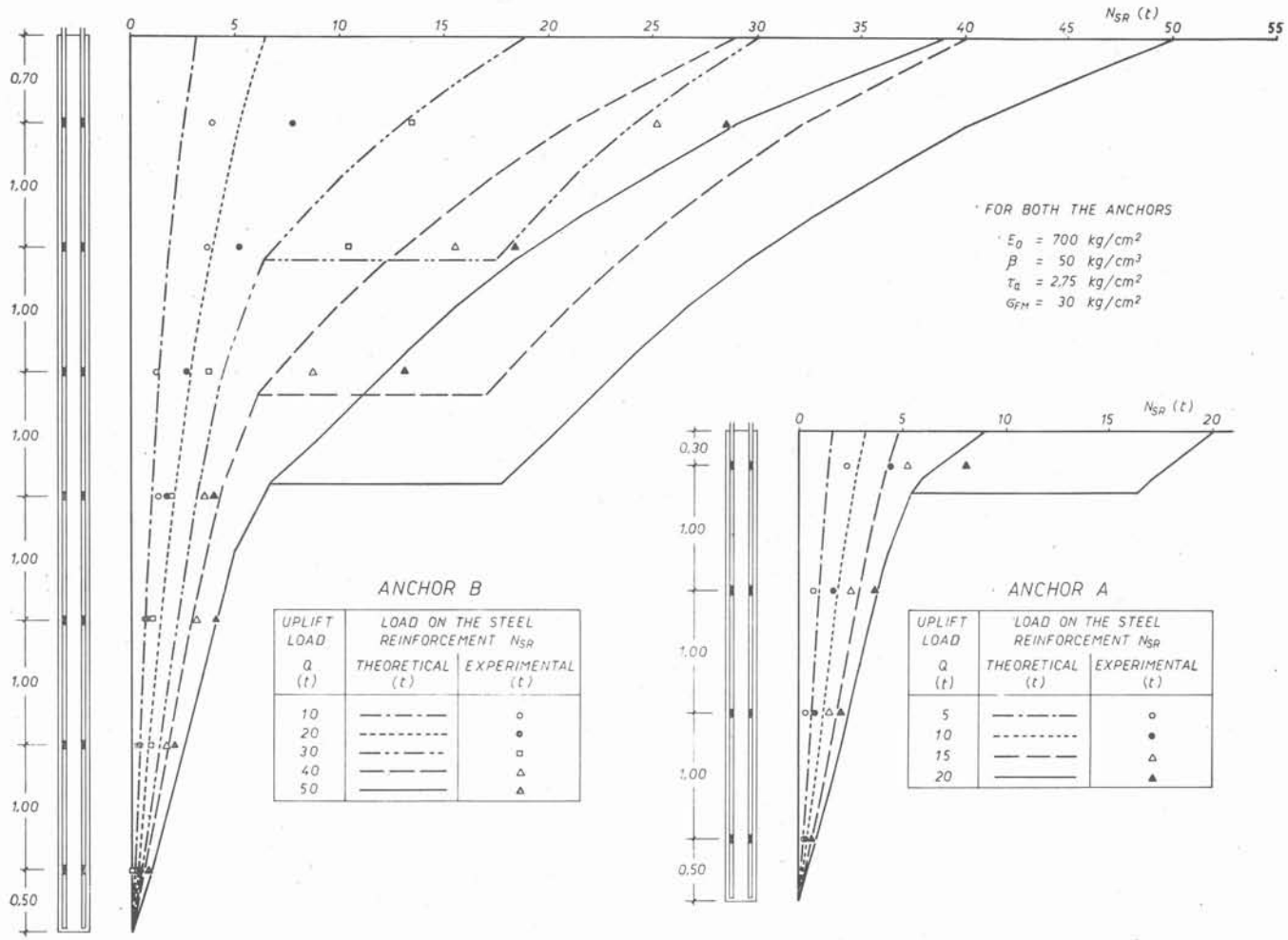

Fig 10. — **Load on steel bars. Comparison between theoretical and experimental values.**

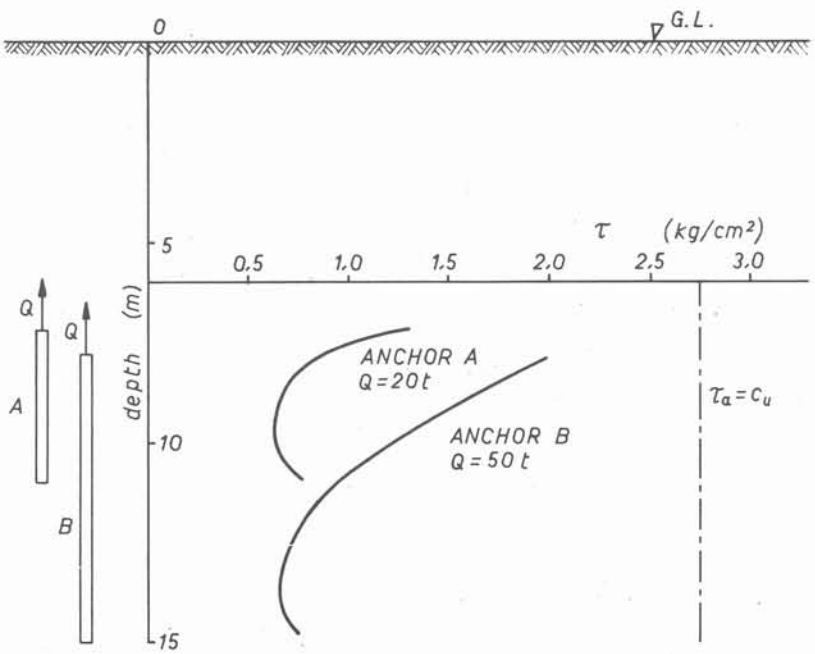

Fig. 11. — **Calculated values of τ at failure.**

The results obtained with such a set of parameters are reported in fig. 10 together with field data; the agreement may be seen to be rather good, except for the points near the anchor top for loads below the values producing tension cracks. Such differences could be explained with a decrease of the modulus E_M in this highy stressed zone.

The value $\tau_a = 2.75$ kg/cm² corresponds to the mean value of undrained cohesion c_u of the soil determined in laboratory, on samples 3, A, B and 6 falling below top levels of the anchors, while the value of $E = 700$ kg/cm² is derived from the same value of c_u following the suggestions of Poulos (1972) for bored piles in clay. The value of $\beta = 50$ kg/cm³ is rather different from the average laboratory value determined by means of shear box tests; in this connexion the differences between laboratory direct shear test on undisturbed samples and the field behaviour of the interface between the mortar and the soil must be recalled.

As already said, the calculations offer the possibility of predicting the load-displacement response of the top of the anchor. With the values of parameters discussed above the initial part of the load-displacement curve is predicted very well; on the contrary, for both anchors, the upheaval at high loads are grossly underestimated and the values of failure load overestimated.

It seems that the usual hypothesis of uniform shear stress $\tau = \alpha\ c_u$ at failure does not depict the actual phenomenon. This is confirmed by the fact that different values of α ($0.28 \div 0.36$) are derived by the three test anchors of different length, but identical in any other respect.

A further confirmation may be obtained from the results of the calculations carried out to determine the stress distribution in the reinforcement bar. In fig. 11, the diagrams of the calculated values of τ at failure are reported for both anchors A and B; it is to be remembered that these shear stresses are compatible with the measured values of the stress in the steel rods. It may be seen that the distribution of τ is far from uniform, and the maximum value is lower than $\tau_a = c_u$. Finally, it is interesting to point out that the pattern of τ, decreasing downwards, is in contrast with the usual interpretation of failure in terms of total stress. It may be argued that an effective stress analysis could be more suited, and could account for some drainage at the interface between the soil and the mortar, due to the relatively high mortar permeability.

In terms of effective stress the shear stress τ becomes a function of the radial normal stress at the interface; it is interesting to point out that, according to Mindlin formulas, the radial stress decreases downwards being compressive at the top and tensile at the bottom of the anchor.

4. CONCLUSIONS

The analysis shows that, taking into account tension cracks in the mortar, it is possible to explain the non linear load variation with depth in the anchor, even at failure.

The same analysis, with the same values of parameters involved, fails in predicting the final part of the load-upheaval curve, and the value of failure load.

Such a discrepancy is probably related to the hypothesis of a uniform distribution of $\tau = \alpha\ c_u$, assumed in the analysis of failure in terms of total stress.

Further theoretical and experimental investigations are needed to elucidate this point; it appears that an interpretation in terms of effective stress could offer considerable advantages.

REFERENCES

ADAMS (J.I.) and KLYM (T.W.). — «A study of anchorages for transmission tower foundations», *Canadian Geotechnical Journal,* Vol. 9, N° 89 (1972).

BERARDI (G.). — «Sul comportamento di ancoraggi immersi in terreni diversi», *Pubblicazioni Istituto di Scienza delle Costruzioni,* Università di Genova, Serie III, N° 60 (1967).

CLOUGH (G.W.) and DUNCAN (J.M.). — «Finite element analysis of retaining wall behavior», *Journal Soil Mech. Founds. Divn.,* Proc. ASCE, Vol. 97, SM 12 (1971).

DESAI (C.). — «Numerical design-analysis for piles in sands», *Journal Geot. Eng. Divn.,* Proc. ASCE, Vol. 100, GT 6 (1974).

EVANGELISTA (A.). — «Pali inclinati isolati ed in gruppo immersi in un mezzo elastico», *Rivista Italiana di Geotecnica,* anno X, N. 3 (1976).

KONDNER (R.L.) and ZELASKO (J.S.). — «A hyperbolic stress-strain formulation for sands», Proc. second. Pan-Am. Conf. Soil Mech. and Found. Eng., Vol. I, Brazil (1963).

MATTES (N.S.) and POULOS (H.G.). — «Settlement of a single compressible pile», *Journal Soil Mech. Founds. Divn.,* Proc. ASCE, Vol. 95, SM 1 (1969).

POULOS (H.G.). — «Load settlement prediction for piles and piers», *Journal Soil Mech. Founds. Divn.,* Proc. ASCE, Vol. 98, SM 9 (1972).

POULOS (H.G.) and DAVIS (E.H.). — «The settlement of behaviour of single axially loaded incompressible piles and piers», *Geotechnique,* Vol. 18, N° 3 (1968).

SAPIO (G.). — «Comportamento di tiranti di ancoraggio in formazioni di argille preconsolidate», Atti XII Convegno Nazionale di Geotecnica, Cosenza, Italy (1975).